Articles

The Importance of a Conformational Equilibrium on the Reactivity of Molybdenum and Rhenium Hydroxo−Carbonyl Complexes toward Phenyl Acetate: A Theoretical Investigation

Violeta Yeguas, Pablo Campomanes, and Ramón López*

Departamento de Química Física y Analítica, Facultad de Química, Universidad de Oviedo, Julián Clavería 8, 33006 Oviedo, Principado de Asturias, Spain

Received March 15, 2007

The reaction of [Mo(OH)(η^3-C_3H_5)(CO)$_2$($N_2C_2H_4$)] and [Re(OH)(CO)$_3$($N_2C_2H_4$)] with phenyl acetate to give phenol and [Mo(OAc)(η^3-C_3H_5)(CO)$_2$($N_2C_2H_4$)] and [Re(OAc)(CO)$_3$($N_2C_2H_4$)], respectively, was investigated by using the B3LYP density functional theory methodology in conjunction with the PCM-UAHF model to take into account solvent effects. For both complexes, the most favorable reaction mechanism is concerted and takes place, for the first time in the metal-promoted ester hydrolysis, through the addition of the complex O−H bond to the ester single C−O bond. The larger reactivity of the Mo complex experimentally found is explained in terms of the interaction detected in the rate-determining TS between one of the lone pairs of the oxygen atom bearing the phenyl group and the two π-antibonding C−N of the bidentate ligand. Due to the existence of a conformational equilibrium for the Mo complex, its reaction with phenyl acetate can evolve through a rate-determining TS 2.4 kcal mol^{-1} lower in relative energy than that found for the Re case, thus explaining the ratio between both periods of experimental reaction time.

Introduction

Carboxylic ester hydrolysis has attracted considerable attention due to its occurrence in many processes of chemistry and biochemistry.[1−7] Most esters do not readily hydrolyze in neutral aqueous solution, and consequently the use of catalysts is required.[4,7] Among them, many ester-hydrolyzing enzymes contain metal ions in their active sites. This fact has provoked numerous studies on the synthesis of metal complexes acting as model compounds for the hydrolytic metalloenzymes,[8−25] thus providing valuable information for understanding the chemistry involved in the action of these metalloenzymes and for designing efficient artificial metalloenzymes. Particularly, these model studies have revealed the mechanisms of action of the metal ions that can be used in these processes.[8,9,13,17,23]

Three basic mechanisms have been proposed to account for the metal-promoted ester hydrolysis (see Scheme 1). In the first, the metal activates a coordinated hydroxide for the intermolecular nucleophilic attack on the ester carbonyl carbon (Scheme 1 (A)).[8,9] In the second case, the metal activates the ester carbonyl carbon atom toward nucleophilic attack by a hydroxide molecule (Scheme 1 (B)).[9,17] The third proposal is a combined mechanism where the metal-OH acts as a nucleophile and at the same time the metal offers an open site for C═O binding (Scheme 1 (C)).[8,9,13,23]

* Corresponding author. Tel: +34 98 5 102 967. Fax: +34 98 5 103 1255. E-mail: rlopez@uniovi.es.

(1) Bender, M. L. *Chem. Rev.* **1960**, *60*, 53.
(2) Jencks, W. P. *Chem. Rev.* **1972**, *72*, 705.
(3) Williams, A. In *Enzyme Mechanism*; Page, M. I., Williams, A., Eds.; Burlington: London, 1987.
(4) Lowry, T. H.; Richardson, K. S. *Mechanism and Theory in Organic Chemistry*, 3rd ed.; Harper and Row: New York, 1987.
(5) Faber, K. *Biotransformations in Organic Chemistry: A Textbook*, 3rd ed.; Springer: Berlin, 1997.
(6) Patel, R. N. *Stereoselective Biocatalysis*; Marcel Dekker: New York, 2000.
(7) Smith, M. B.; March, J. *March's Advanced Organic Chemistry: Reactions, Mechanisms, and Structure*, 6th ed.; Wiley-Interscience: New York, 2007.
(8) Chin, J. *Acc. Chem. Res.* **1991**, *24*, 145.
(9) Koike, T.; Kimura, K. *J. Am. Chem. Soc.* **1991**, *113*, 8935.
(10) Looney, A.; Parkin, G.; Alsfasser, R.; Ruf, M.; Vahrenkamp, H. *Angew. Chem., Int. Ed. Engl.* **1992**, *31*, 92.
(11) Ruf, M.; Weis, K.; Vahrenkamp, H. *J. Chem. Soc., Chem. Commun.* **1994**, 135.
(12) Koike, T.; Kajitani, S.; Nakamura, I.; Kimura, E.; Shiro, M. *J. Am. Chem. Soc.* **1995**, *117*, 1210.
(13) Ruf, M.; Vahrenkamp, H. *Chem. Ber.* **1996**, *129*, 1025.
(14) Frey, S. T.; Murthy, N. N.; Weintraub, S. T.; Thompson, L. K.; Karlin, K. D. *Inorg. Chem.* **1997**, *36*, 956.
(15) Bazzicalupi, C.; Bencini, A.; Bianchi, A.; Fusi, V.; Giorgi, C.; Paoletti, P.; Valtancoli, B.; Zanchi, D. *Inorg. Chem.* **1997**, *36*, 2784.
(16) Kimura, E.; Koike, T. *Chem. Commun.* **1998**, 1495.
(17) Suh, J.; Son, S. J.; Suh, M. P. *Inorg. Chem.* **1998**, *37*, 4872.
(18) Yin, X.; Lin, C.; Zhou, Z.; Chen, W.; Zhu, S.; Lin, H.; Su, X.; Chen, Y. *Transition Met. Chem.* **1999**, *24*, 537.
(19) Bazzicalupi, C.; Bencini, A.; Berni, E.; Bianchi, A.; Fedi, V.; Fusi, V.; Giorgi, C.; Paoletti, P.; Valtancoli, B. *Inorg. Chem.* **1999**, *38*, 4115.
(20) Bencini, A.; Berni, E.; Bianchi, A.; Giorgi, C.; Paoletti, P.; Valtancoli, B.; Zanchi, D. *Inorg. Chem.* **1999**, *38*, 6323.
(21) Xia, J.; Xu, Y.; Li, S.; Sun, W.; Yu, K.; Tang, W. *Inorg. Chem.* **2001**, *40*, 2394.
(22) Li, S.; Xia, J.; Yang, D.; Xu, Y.; Li, D.; Wu, M.; Tang, W. *Inorg. Chem.* **2002**, *41*, 1807.
(23) DiTargiani, R. C.; Chang, S.; Salter, M. H.; Hancock, R. D.; Goldberg, D. P. *Inorg. Chem.* **2003**, *42*, 5825.
(24) Kou, X.; Meng, X.; Xie, J.; Zeng, X. *Transition Met. Chem.* **2003**, *28*, 777.
(25) Huang, J.; Li, D.; Li, S.; Yang, D.; Sun, W.; Tang, W. *J. Inorg. Biochem.* **2004**, *98*, 502.

10.1021/om0702431 CCC: $37.00
Publication on Web 09/26/2007

Scheme 1. Mechanistic Proposals for the Metal-Promoted Ester Hydrolysis[a]

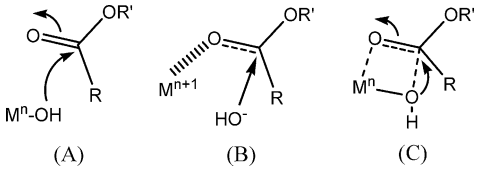

[a] The superscript n indicates the charge on the metal (M).

The synthesis of organometallic hydroxo compounds is important not only in relation to hydrolytic metalloenzymes but also due to their rich OH-centered reactivity,[26] which is dominated by the nucleophilic character of the hydroxo ligand. In the last years, the chemistry of hydroxo complexes of middle (groups 6 and 7) transition-metal fragments has started to be explored.[26−34] Recent experimental studies have reported the synthesis of the [Mo(OH)(η^3-C_3H_4-Me-2)$(CO)_2$(phen)] and [Re(OH)$(CO)_3$(Me_2-bpy)] complexes[27,28,32] and their reactivity toward esters and other organic electrophiles.[31,32,34] It is interesting to note that the reactivity of the molybdenum hydroxo−carbonyl complex toward phenyl acetate is larger than that of the rhenium hydroxo−carbonyl complex.[32] The former reaction is complete in 8 h at room temperature in dichloromethane solution, while the latter one needs 20 h.

We present here the first theoretical mechanistic study of the reaction of [Mo(OH)(η^3-C_3H_5)$(CO)_2$(N−N)] and [Re(OH)$(CO)_3$(N−N)] (N−N = HN═CH−CH═NH) with phenyl acetate to afford [Mo(OAc)(η^3-C_3H_5)$(CO)_2$(N−N)] and [Re(OAc)$(CO)_3$(N−N)], respectively, and phenol, trying to gain information on the factors that govern the reactivity experimentally observed.

Computational Details

The computational investigation was performed with the simplified complexes [Mo(OH)(η^3-C_3H_5)$(CO)_2$(HN═CH−CH═NH)] and [Re(OH)$(CO)_3$(HN═CH−CH═NH)], which were chosen to mimic the ones experimentally used and to minimize the computational time. In particular, theoretical studies on the formation of β-lactams from an *N*-rhenaimine and the catalytic reduction of acetone by a rhodium complex have proved the adequacy of replacing the bipyridine (bpy) ligand by the diimine (HN═CH−CH═NH) one.[35]

Quantum chemical computations were carried out with the Gaussian 03 series of programs.[36] Full geometry optimizations of stable species and transition states (TS) were performed in the gas phase by employing the hybrid density functional B3LYP[37] with the 6-31+G(d,p) basis set[38] (LANL2DZ for Mo and Re atoms augmented by f polarization functions with exponents 1.043 and 0.869, respectively)[39] and by using the standard Schlegel algorithm.[40] The B3LYP functional combines Becke's three-parameter nonlocal hybrid exchange potential with the nonlocal correlation functional of Lee, Yang, and Parr. The nature of the stationary points was verified by analytical computations of harmonic vibrational frequencies. Intrinsic reaction coordinate (IRC) calculations with the Gonzalez and Schlegel method[41] were carried out to check the two minimum energy structures connecting each TS.

To take into account condensed-phase effects, single-point calculations were also performed on the gas-phase-optimized geometries using the polarizable continuum model (PCM) of Tomasi et al.[42] with the united atom Hartree−Fock (UAHF) parametrization.[43] The energy in solution comprises the electronic energy of the polarized solute, the electrostatic solute−solvent interaction energy $\langle\Psi_f|H + 1/2V_f|\Psi_f\rangle$, and the nonelectrostatic terms corresponding to cavitation, dispersion, and short-range repulsion. A relative permittivity of 8.93 was assumed in the calculations to simulate dichloromethane as the solvent experimentally used.

To check the reliability of our computational scheme, we also optimized at the B1B95/SDB-aug-cc-pVDZ[44,45] level of theory the key critical structures involved in the most favorable mechanisms previously found at the B3LYP level of theory.[46−48] The former computational scheme has been reported to perform remarkably well for late-transition-metal reactions, giving rise to results near CCSD(T) quality.[49] Bulk solvent effects were also taken into account by using the PCM-UAHF method as in the B3LYP case. According to our B1B95 results, the small energy differences found at the B3LYP level of theory between the most significant TS involved in the most favorable reaction mechanisms located remain qualitatively unchanged (see Results and Discussion section). In addition, the comparison of the B1B95 geometries for the complexes [Mo(OH)(η^3-C_3H_5)$(CO)_2$(HN═CH−CH═NH)] and [Re(OH)$(CO)_3$(HN═CH−CH═NH)] with the X-ray diffraction experimental ones[28,29] shows similar maximum relative deviations (5.1% for bond distances

(26) Fulton, J. R.; Holland, A. W.; Fox, D. J.; Bergman, R. G. *Acc. Chem. Res.* **2002**, *35*, 44.
(27) Gibson, D. H.; Yin, X. *J. Am. Chem. Soc.* **1998**, *120*, 11200.
(28) Morales, D.; Clemente, M. E. N.; Pérez, J.; Riera, L.; Riera, V.; Miguel, D. *Organometallics* **2002**, *21*, 4934.
(29) Gibson, D. H.; Yin, X.; Hen, H.; Mashuta, M. S. *Organometallics* **2003**, *22*, 337.
(30) Heard, P. J.; Sroisuwan, P.; Tocher, D. A. *Polyhedron* **2003**, *22*, 1321.
(31) Gerbino, D. C.; Hevia, E.; Morales, D.; Clemente, M. E. N.; Pérez, J.; Riera, L.; Riera, V.; Miguel, D. *Chem. Commun.* **2003**, 328.
(32) Cuesta, L.; Gerbino, D. C.; Hevia, E.; Morales, D.; Navarro-Clemente, M. E.; Pérez, J.; Riera, L.; Riera, V.; Miguel, D.; Del Río, I.; García-Granda, S. *Chem.−Eur. J.* **2004**, *10*, 1765.
(33) Breno, K. L.; Pluth, M. D.; Landorf, C. W.; Tyler, D. R. *Organometallics* **2004**, *23*, 1738.
(34) Cuesta, L.; Hevia, E.; Morales, D.; Pérez, J.; Riera, L.; Miguel, D. *Organometallics* **2006**, *25*, 1717.
(35) (a) Hevia, E.; Pérez, J.; Riera, V.; Miguel, D.; Campomanes, P.; Menéndez, M. I.; Sordo, T. L.; García-Granda, S. *J. Am. Chem. Soc.* **2003**, *125*, 3706. (b) Iron, M. A.; Sundermann, A.; Martin, J. M. L. *J. Am. Chem. Soc.* **2003**, *125*, 11430.
(36) Frisch, M. J.; et al. *Gaussian 03*, Revision C.02; Gaussian, Inc.: Wallingford, CT, 2004.
(37) (a) Becke, A. D. *Phys. Rev. A* **1988**, *38*, 3098. (b) Lee, C.; Yang, W.; Parr, R. G. *Phys. Rev. B* **1988**, *37*, 785. (c) Becke, A. D. *J. Chem. Phys.* **1993**, *98*, 5648.
(38) Hehre, W. J.; Radom, L.; Pople, J. A.; Schleyer, P. V. R. *Ab Initio Molecular Orbital Theory*; Wiley: New York, 1986.
(39) (a) Hay, P. J.; Wadt, W. R. *J. Chem. Phys.* **1985**, *82*, 299. (b) Ehlers, A. W.; Böhme, M.; Dapprich, S.; Gobbi, A.; Höllwarth, A.; Jonas, V.; Köhler, K. F. *Chem. Phys. Lett.* **1993**, *208*, 111.
(40) Schlegel, H. B. *J. Comput. Chem.* **1982**, *3*, 214.
(41) (a) Gonzalez, C.; Schlegel, H. B. *J. Phys. Chem*. **1989**, *90*, 2154. (b) Gonzalez, C.; Schlegel, H. B. *J. Phys. Chem*. **1990**, *94*, 5523.
(42) (a) Tomasi, J.; Persico, M. *Chem. Rev.* **1994**, *94*, 2027. (b) Tomasi, J.; Cammi, R. *J. Comput. Chem.* **1995**, *16*, 1449.
(43) Barone, V.; Cossi, M.; Tomasi, J. *J. Chem. Phys.* **1997**, *107*, 3210.
(44) The B1B95 functional combines Becke GGA exchange, 28% Hartree−Fock exchange, and the Becke95 meta-GGA correlation functional (see ref 46).
(45) The SDB-aug-cc-pVDZ basis set combines the Dunning aug-cc-pVDZ basis set (see ref 47) on the main-group elements and the Stuttgart−Dresden basis set−RECP combination on the Mo and Re atoms with an added f-type polarization exponent (see ref 48).
(46) Becke, A. D. *J. Chem. Phys.* **1996**, *104*, 1040.
(47) (a) Dunning, T. H., Jr. *J. Chem. Phys.* **1989**, *90*, 1007. (b) Kendall, R. A.; Dunning, T. H., Jr.; Harrison, R. J. *J. Chem. Phys.* **1992**, *96*, 6796. (c) Woon, D. E.; Dunning, T. H., Jr. *J. Chem. Phys.* **1993**, *98*, 1358.
(48) Iron, M. A.; Lucassen, A. C. B.; Cohen, H.; van der Boom, M. E.; Martin, J. M. L. *J. Am. Chem. Soc.* **2004**, *126*, 11699, and references therein.
(49) Quintal, M. M.; Karton, A.; Iron, M. A.; Boese, A. D.; Martin, J. M. L. *J. Phys. Chem. A* **2006**, *110*, 709.

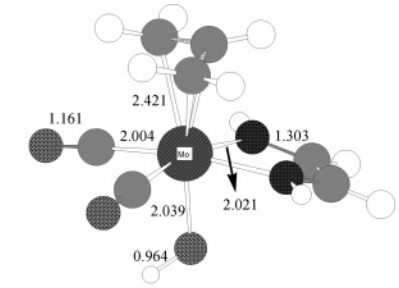

$[Mo(OH)(\eta^3\text{-}C_3H_5)(CO)_2(N_2C_2H_4)]$, (**R**)

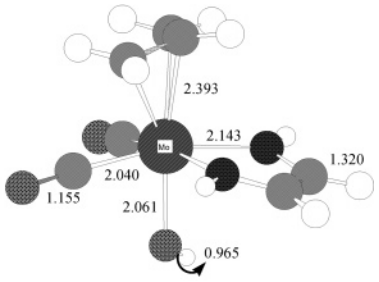

TS$_{rot}$-Mo

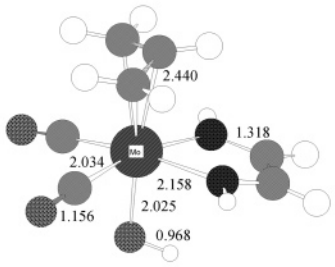

$[Mo(OH)(\eta^3\text{-}C_3H_5)(CO)_2(N_2C_2H_4)]$, (**R'**)

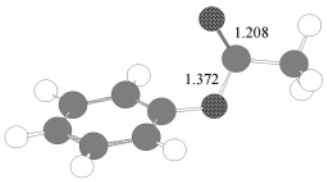

phenyl acetate

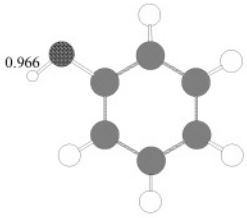

phenol

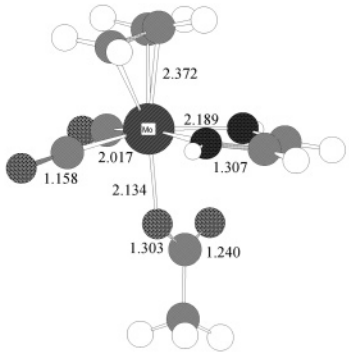

$[Mo(OAc)(\eta^3\text{-}C_3H_5)(CO)_2(N_2C_2H_4)]$

Figure 1. B3LYP/6-31+G(d,p) (LANL2DZ for Mo augmented by f polarization functions with exponent 1.043) optimized geometries of the reactants, TS for the interconversion of the two conformers of the Mo complex, and products involved in the reaction of $[Mo(OH)(\eta^3\text{-}C_3H_5)(CO)_2(N_2C_2H_4)]$ toward phenyl acetate.

and 6.4% for bond angles) to those found in the B3LYP case (4.9% and 6.9%, respectively). Thus, these results confirm the validity of our B3LYP mechanistic predictions.

For interpretation purposes, a natural bond orbital (NBO) analysis was performed on some of the most important critical structures along the reaction coordinates at the B3LYP level of theory.[50] A topological analysis of the electronic charge density, ρ, was also carried out using the atoms-in-molecules (AIM) theory of Bader.[51] This analysis was performed using the AIMPAC program package.[52]

Results and Discussion

We will present first the results obtained for the reaction between $[Mo(OH)(\eta^3\text{-}C_3H_5)(CO)_2(N_2C_2H_4)]$ and phenyl acetate to give $[Mo(OAc)(\eta^3\text{-}C_3H_5)(CO)_2(N_2C_2H_4)]$ and phenol, and then those for the reaction between $[Re(OH)(CO)_3(N_2C_2H_4)]$ and phenyl acetate to yield $[Re(OAc)(CO)_3(N_2C_2H_4)]$ and phenol. Unless otherwise stated, we will discuss in the text the energies in CH_2Cl_2 solution.

Reaction between $[Mo(OH)(\eta^3\text{-}C_3H_5)(CO)_2(N_2C_2H_4)]$ and Phenyl Acetate. The $[Mo(OH)(\eta^3\text{-}C_3H_5)(CO)_2(N_2C_2H_4)]$ complex can exist in two different isomeric forms depending on the orientation of the OH ligand (see **R** and **R′** in Figure 1). The most stable isomer, **R** (0.0 kcal mol^{-1}), presents the H atom of the hydroxyl ligand oriented opposite the $N_2C_2H_4$ ligand, while in the less stable one, **R′** (0.8 kcal mol^{-1}), this H atom is oriented toward the bidentate ligand. Both isomers are connected by means of a rotational TS, **TS$_{rot}$-Mo**, with an energy barrier in solution of 4.3 kcal mol^{-1} (see Figure 1). Therefore, starting from **R** + AcOPh, the process can undergo an isomerization step followed by the reaction of **R′** with the ester or proceed directly through the reaction between **R** and the ester. The reaction of each isomer of the Mo complex with phenyl acetate can evolve through three different reaction mechanisms: one concerted and two stepwise ones. As the reaction pathways from **R′** + AcOPh are more stable than the analogous ones from **R** + AcOPh, we will discuss first the former ones. Figures 2 and

(50) (a) Reed, E.; Curtiss, L. A.; Weinhold, F. *Chem. Rev.* **1988**, *88*, 899. (b) Weinhold, F.; Carpenter, J. E. In *The Structure of Small Molecules and Ions*; Naaman, R., Vager, Z., Eds.; Plenum Press: New York, 1988.

(51) Bader, R. F. W. *Atoms in Molecules. A Quantum Theory*; Clarendon: Oxford, 1990.

(52) Biegler-Konig, F. W.; Bader, R. F. W.; Hua-Tang, T. *J. Comput. Chem.* **1982**, *3*, 317.

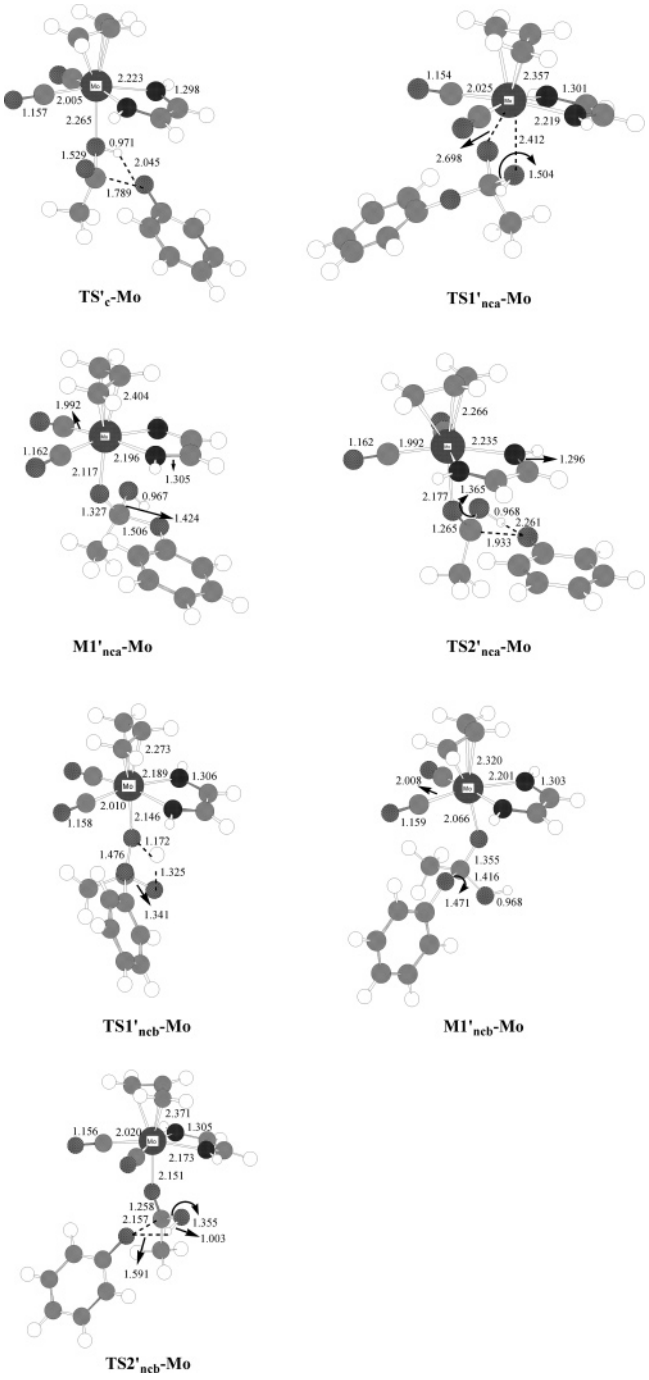

Figure 2. B3LYP/6-31+G(d,p) (LANL2DZ for Mo augmented by f polarization functions with exponent 1.043) optimized geometries of the most chemically significant intermediates and TSs involved in the reaction of $[Mo(OH)(\eta^3\text{-}C_3H_5)(CO)_2(N_2C_2H_4)]$ toward phenyl acetate.

3 collect the located critical structures involved in them (see also Figure 1 for the products) and the corresponding energy profiles in solution, respectively.

The concerted pathway evolves through a TS, **TS′$_c$-Mo**, (26.6 kcal mol^{-1}), for the nucleophilic attack of the hydroxyl O atom of the complex to the carbonyl C atom of the ester fragment and simultaneous transfer from the hydroxyl H atom to the noncarbonyl O atom of the ester. At this TS the hydroxyl O−H bond is slightly elongated (0.971 Å) and the original C−O$_{phenoxide}$ bond of the ester moiety is practically broken (1.789 Å), whereas two new bonds start to form, the O$_{hydroxyl}$−C$_{carbonyl}$ bond (1.529 Å) and the H$_{hydroxyl}$−O$_{phenoxide}$ bond (2.045 Å). **TS′$_c$-Mo** connects **R′** + AcOPh with the separate products, $[Mo(OAc)(\eta^3\text{-}C_3H_5)(CO)_2(N_2C_2H_4)]$ and phenol, 12.2 kcal mol^{-1} more stable than the separate reactants, **R** + AcOPh. One of the stepwise mechanisms proceeds through a TS, **TS1′$_{nca}$-Mo** (27.9 kcal mol^{-1}), which involves an initial attack of the OH ligand on the carbonyl C atom with simultaneous coordination of one of the ester O atoms to the metal center to give an intermediate, **M1′$_{nca}$-Mo**, (12.9 kcal mol^{-1}). At this intermediate, the Mo atom is linked to the carbonyl O atom at a distance of 2.117 Å, while the hydroxyl O atom is linked to the carbonyl C atom (1.424 Å). Then, **M1′$_{nca}$-Mo** renders the separate products through the TS **TS2′$_{nca}$-Mo** (16.7 kcal mol^{-1}) for the cleavage of the C$_{carbonyl}$−O$_{phenoxide}$ bond (1.993 Å) and simultaneous H migration from the hydroxyl O atom to the phenoxide O atom. Therefore, the rate-determining step of this mechanism is the first one, with an energy barrier in solution of 27.9 kcal mol^{-1}. This route corresponds to the mechanistic proposal type C in Scheme 1. Along the third route the system evolves through a TS, **TS1′$_{ncb}$-Mo**, with an energy barrier of 42.3 kcal mol^{-1} for the addition of the OH ligand on the carbonyl double bond of the ester to yield an intermediate, **M1′$_{ncb}$-Mo** (11.3 kcal mol^{-1}). At this intermediate, the hydroxyl O atom is linked to the carbonyl C atom at a distance of 1.476 Å, whereas the original hydroxyl H atom is transferred to the initial carbonyl O atom (0.968 Å). **M1′$_{ncb}$-Mo** leads to the final products through the TS **TS2′$_{ncb}$-Mo** (22.3 kcal mol^{-1}) for eliminating the phenoxide fragment and placing the H atom previously transferred to the carbonyl O atom of the ester onto the O atom of the phenoxide fragment. Therefore, according to these results, the first step of this mechanism is the rate-determining one and presents a high energy barrier in solution of 42.3 kcal mol^{-1}. This reaction mechanism is similar to the mechanistic proposal type A in Scheme 1.

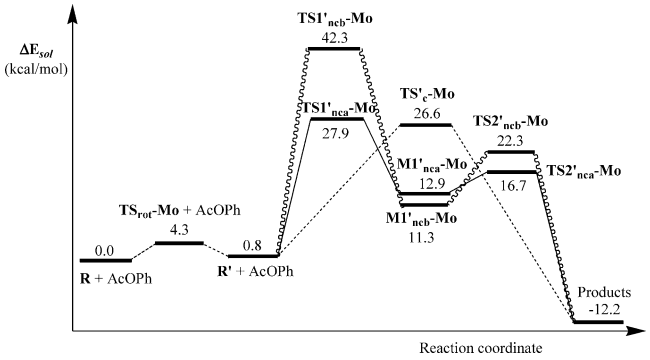

Figure 3. B3LYP/6-31+G(d,p) (LANL2DZ for Mo augmented by f polarization functions with exponent 1.043) energy profiles in solution located for the reaction of $[Mo(OH)(\eta^3\text{-}C_3H_5)(CO)_2(N_2C_2H_4)]$ toward phenyl acetate.

As mentioned above, **R** can directly interact with phenyl acetate along analogous mechanisms to those just described but with higher energy barriers in solution: 31.2 kcal mol^{-1} for the concerted mechanism, 28.3 kcal mol^{-1} for the first stepwise route, and 44.7 kcal mol^{-1} for the second stepwise one. Figure 1S and Table 1S in the Supporting Information collect the corresponding optimized geometries and energies, respectively.

In connection with the mechanism type B previously shown in Scheme 1, wherein the metal binds to the carbonyl O atom while the hydroxide group attacks the carbonyl C atom, we also investigated the cleavage of the metal−OH bond by optimizing the structures corresponding to $[Mo(\eta^3\text{-}C_3H_5)(CO)_2(N_2C_2H_4)]^+$ and OH$^-$ (see Table 4S in the Supporting Information). According to our results, this process is very unstable given

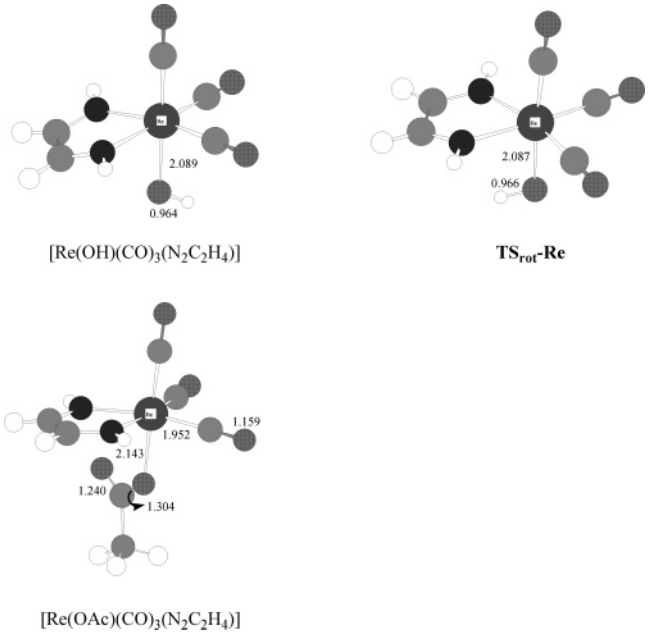

Figure 4. B3LYP/6-31+G(d,p) (LANL2DZ for Re augmented by f polarization functions with exponent 0.869) optimized geometries of the $[Re(OH)(CO)_3(N_2C_2H_4)]$ reactant, the TS for the interconversion of this complex into its mirror image, and the $[Re(OAc)(CO)_3(N_2C_2H_4)]$ product.

that $[Mo(\eta^3\text{-}C_3H_5)(CO)_2(N_2C_2H_4)]^+ + OH^-$ are 61.0 kcal mol^{-1} higher in energy in solution than **R**.

Therefore, our results indicate that the most favorable reaction mechanism for the reaction between $[Mo(OH)(\eta^3\text{-}C_3H_5)(CO)_2(N_2C_2H_4)]$ and phenyl acetate evolves through the **R′** conformer and presents an energy barrier of 26.6 kcal mol^{-1} (**TS′$_c$-Mo**). However, the rate-determining TSs for the second (**TS1′$_{nca}$-Mo**) and third (**TS1$_{nca}$-Mo**) most favorable reaction mechanisms are only 1.3 and 1.7 kcal mol^{-1}, respectively, above **TS′$_c$-Mo**. PCM-B1B95/SDB-aug-cc-pVDZ calculations predict the same trend in the mechanistic proposals, the energy differences between **TS1′$_{nca}$-Mo** and **TS′$_c$-Mo** and between **TS1$_{nca}$-Mo** and **TS′$_c$-Mo** being now 0.6 and 1.8 kcal mol^{-1}, respectively (see Tables 5S and 6S in the Supporting Information).

Reaction between [Re(OH)(CO)$_3$(N$_2$C$_2$H$_4$)] and Phenyl Acetate. For the $[Re(OH)(CO)_3(N_2C_2H_4)]$ complex only a minimum energy conformation was located and it corresponds to the hydroxyl H atom oriented opposite the $N_2C_2H_4$ ligand (see Figure 4). In contrast with the Mo case, the structure in which the hydroxyl H atom is oriented toward the bidentate ligand is now a TS, **TS$_{rot}$-Re**, 3.6 kcal mol^{-1} less stable than the Re complex (see Figure 4). The Re complex can react with phenyl acetate through three reaction mechanisms analogous to those found for the **R** conformer of $[Mo(OH)(\eta^3\text{-}C_3H_5)(CO)_2(N_2C_2H_4)]$. Figures 5 and 6 display the critical structures located along them (see also Figure 4 for the $[Re(OAc)(CO)_3(N_2C_2H_4)]$ product) and the corresponding energy profiles in solution, respectively.

The concerted TS, **TS$_c$-Re**, presents now an energy barrier in solution of 29.0 kcal mol^{-1}. At this TS the hydroxyl O−H bond is slightly elongated (0.984 Å) and the original $C-O_{phenoxide}$ bond of the ester moiety is clearly broken (2.015 Å), whereas two new bonds start to form, the $O_{hydroxyl}-C_{carbonyl}$ bond (1.477 Å) and the $H_{hydroxyl}-O_{phenoxide}$ bond (1.827 Å). It is interesting to note that the interaction between both reactants at **TS$_c$-Re** takes place at similar distances to those at **TSc-Mo** (see Figure 1S in the Supporting Information) but at shorter

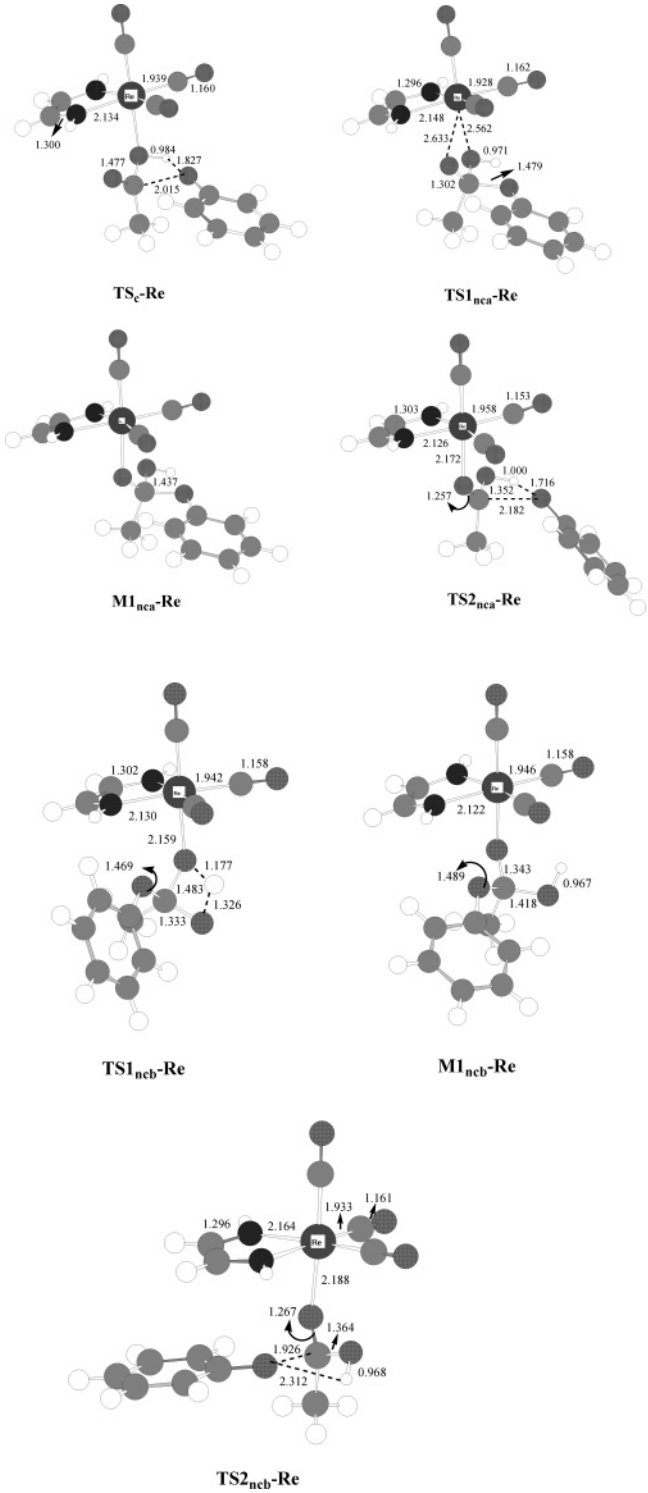

Figure 5. B3LYP/6-31+G(d,p) (LANL2DZ for Re augmented by f polarization functions with exponent 0.869) optimized geometries of the most chemically significant intermediates and TSs involved in the reaction of $[Re(OH)(CO)_3(N_2C_2H_4)]$ toward phenyl acetate.

distances than at **TS′$_c$-Mo** (see Figures 3 and 6). The rate-determining step along the first nonconcerted route is, as in the case of the Mo complex, the first one that corresponds to the formal insertion of the ester into the $Re-O_{hydroxyl}$ bond. The corresponding TS is **TS1$_{nca}$-Re**, with an energy barrier in solution of 30.7 kcal mol^{-1}. The rate-determining TS along the second stepwise mechanism is the first one, **TS1$_{ncb}$-Re**, and presents a high energy barrier in solution of 42.6 kcal mol^{-1}. The final products, $[Re(OAc)(CO)_3(N_2C_2H_4)]$ + phenol (see

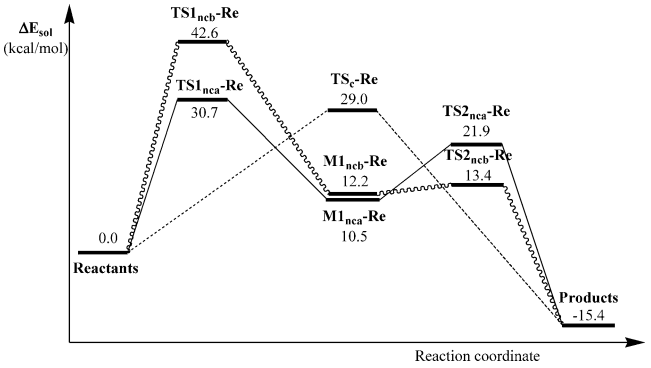

Figure 6. B3LYP/6-31+G(d,p) (LANL2DZ for Re augmented by f polarization functions with exponent 0.869) energy profiles in solution located for the reaction of $[Re(OH)(CO)_3(N_2C_2H_4)]$ toward phenyl acetate.

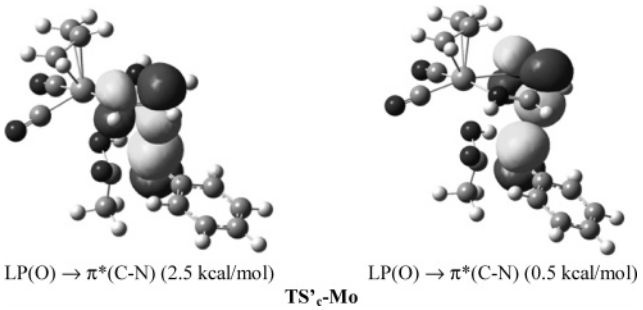

Figure 7. Plot of the "donor−aceptor" (bond−antibond) interactions in the NBO basis for the rate-determining TS of the reaction between $[Mo(OH)(\eta^3\text{-}C_3H_5)(CO)_2(N_2C_2H_4)]$ and phenyl acetate. The corresponding second-order perturbation energies, in kcal mol^{-1}, are also included in parentheses.

Figure 4), are now 15.4 kcal mol^{-1} more stable than separate reactants. Finally, as in the Mo case, the cleavage of the metal−OH bond in the Re complex is a very unstable process given that $[Re(CO)_3(N_2C_2H_4)]^+ + OH^-$ is 65.9 kcal mol^{-1} higher in energy in solution than $[Re(OH)(CO)_3(N_2C_2H_4)]$.

As for $[Mo(OH)(\eta^3\text{-}C_3H_5)(CO)_2(N_2C_2H_4)]$, the reaction between $[Re(OH)(CO)_3(N_2C_2H_4)]$ and phenyl acetate proceeds most favorably through a concerted route with an energy barrier of 29.0 kcal mol^{-1} (**TS$_c$-Re**), although the second most favorable one is 1.7 kcal mol^{-1} (**TS1$_{nca}$-Re**) above the concerted one. PCM-B1B95/SDB-aug-cc-pVDZ calculations reproduce again the same tendency in the mechanistic predictions, the energy difference between **TS1$_{nca}$-Re** and **TS$_c$-Re** being now 0.9 kcal mol^{-1} (see Tables 5S and 6S in the Supporting Information).

Discussion and Comparison with Experiment. According to our theoretical results the reactions of $[Mo(OH)(\eta^3\text{-}C_3H_5)(CO)_2(N_2C_2H_4)]$ and $[Re(OH)(CO)_3(N_2C_2H_4)]$ with phenyl acetate in CH_2Cl_2 solution proceed most favorably through a concerted mechanism, which corresponds to the addition of the hydroxyl O−H bond of the complex to the ester C−O$_{phenoxide}$ bond. To the best of our knowledge, this reaction mechanism had never been reported for the metal-promoted ester hydrolysis. Although it had been considered in some experimental and theoretical studies on the alkaline[53] and neutral[54] hydrolysis of esters in the absence of metal catalysts, the concerted pathway has been found as the most favorable one only for RCOOR′ esters with strong OR′ leaving groups.[55]

The rate-determining concerted TS, **TS′$_c$-Mo**, for the Mo case presents an energy barrier in solution of 26.6 kcal mol^{-1}, while that for the Re one, **TS$_c$-Re**, is 29.0 kcal mol^{-1}, which is in agreement with the larger reactivity of the Mo complex toward phenyl acetate experimentally found.[32] This difference in the energy barriers can be rationalized in terms of an NBO analysis of **TS′$_c$-Mo**. As can be seen in Figure 7, at **TS′$_c$-Mo** the orientation of the OH ligand determines the interaction between one of the lone pairs of the ester O atom bearing the phenyl group and the two π-antibonding C−N of the bidentate ligand with a second-order perturbation energy of 3.0 kcal mol^{-1}. This stabilizing interaction is also shown through the existence of a bond critical point between that O atom and the bidentate ligand with values of the electron density and Laplacian of electron density of 0.014 e Å^{-3} and 0.044 e Å^{-5}, respectively. At **TS$_c$-Re** the orientation of the OH ligand is opposite the bidentate ligand and, therefore, does not allow the interaction mentioned above. In agreement with this, **TS′$_c$-Mo** stabilizes before **TS$_c$-Re** along the corresponding reaction coordinate, thus explaining why the distances involved in the addition of the hydroxyl O−H bond to the ester C$_{carbonyl}$−O$_{phenoxide}$ bond are more stretched at the former TS than at the latter one.

The rate-determining energy barriers obtained in this work, 26.6 and 29.0 kcal mol^{-1}, are closer to that found for the neutral hydrolysis of phenyl acetate (27.2 kcal mol^{-1})[56] than the one for the alkaline hydrolysis of phenyl acetate (12.6 kcal mol^{-1}).[57] This seems to indicate that the nucleophilic character of the OH ligand in the metal complexes studied is similar to that in water.

Finally, it seems worth mentioning that the existence of the **R′** conformer for the Mo complex allows the reaction between this complex and phenyl acetate to proceed through **TS′$_c$-Mo** with an energy barrier in solution 2.4 kcal mol^{-1} (3.1 kcal mol^{-1} at the PCM-B1B95/SDB-aug-cc-pVDZ level of theory) lower than that corresponding to the Re case. This energy difference allows us to explain the difference in the periods of experimental reaction time (8 vs 20 h).[32]

In summary, our theoretical results show that the reactions $[Mo(OH)(\eta^3\text{-}C_3H_5)(CO)_2(N_2C_2H_4)]$ + AcOPh → $[Mo(OAc)(\eta^3\text{-}C_3H_5)(CO)_2(N_2C_2H_4)]$ + PhOH and $[Re(OH)(CO)_3(N_2C_2H_4)]$ + AcOPh → $[Re(OAc)(CO)_3(N_2C_2H_4)]$ + PhOH in dichloromethane solution take place in a concerted manner through the addition of the OH ligand of the organometallic complex to the single C−O bond of the ester. The interaction detected in the rate-determining TS for the Mo case between one of the lone pairs of the ester oxygen atom bearing the phenyl group and the two π-antibonding C−N of the bidentate ligand explains the larger reactivity of the Mo complex toward phenyl acetate in accordance with experimental findings. Furthermore, the conformational equilibrium found for the Mo complex plays an important role by favoring the reaction of this complex with phenyl acetate through an energy barrier in solution that is 2.4 kcal mol^{-1} lower than that for the reaction between the Re complex and phenyl acetate. This explains the ratio between the two periods of reaction time experimentally observed.

(53) (a) Pliego, J. R., Jr.; Riveros, J. M. *Chem.−Eur. J.* **2002**, *8*, 1945 (see also references therein). (b) Pliego, J. R., Jr.; Riveros, J. M. *J. Phys. Chem. A* **2004**, *108*, 2520.

(54) Yamabe, S.; Tsuchida, N.; Hayashida, Y. *J. Phys. Chem. A* **2005**, *109*, 7216.

(55) (a) Ba-Saif, S.; Luthra, A. K. *J. Am. Chem. Soc.* **1989**, *111*, 2647. (b) Williams, A. *Acc. Chem. Res.* **1989**, *22*, 387. (c) Guthrie, J. P. *J. Am. Chem. Soc.* **1991**, *113*, 3941. (d) Hengge, A. C.; Hess, R. A. *J. Am. Chem. Soc.* **1994**, *116*, 11256. (e) Fernandez, M. A.; de Rossi, R. H. *J. Org. Chem.* **1999**, *64*, 6000.

(56) Bowden, K.; Izadi, J.; Powell, S. L. *J. Chem. Res., Synop.* **1997**, 404. An experimental energy barrier in solution of 28.4 kcal mol^{-1} was also reported: Skrabal, A.; Wissensch, w. M d. A. d.; Zahorka, A. *Monatsh. Chem.* **1929**, *54*, 62.

(57) Tommila, E.; Hinshelwood, C. N. *J. Chem. Soc.* **1938**, 1801.

Therefore, our theoretical results could be of interest in designing other organometallic complexes to carry out the ester hydrolysis in milder reaction conditions than those required in the neutral hydrolysis and without having to add aggressive reagents as in the case of alkaline hydrolysis.

Acknowledgment. Financial support from the Ministerio de Educación y Ciencia of Spain (project and grant CTQ2004-06309) is highly appreciated. We also thank Dr. Julio Pérez for useful discussions.

Supporting Information Available: Absolute electronic energies and relative electronic energies, Gibbs energies of solvation, and energies in solution of all the structures presented in this work, imaginary vibrational frequencies corresponding to all the located transition states, Cartesian coordinates corresponding to all the located structures, B3LYP/6-31+G(d,p) (LANL2DZ for Mo augmented by f polarization functions with exponent 1.043) optimized geometries of the intermediates and transition states involved in the reaction of the **R** conformer of [Mo(OH)(η^3-C_3H_5)$(CO)_2$-($N_2C_2H_4$)] toward phenyl acetate without passing through the **R′** conformer, B1B95/SDB-aug-cc-pVDZ Cartesian coordinates and energy data corresponding to reactants and the key transition states involved in the most favorable reaction mechanisms found at the B3LYP level of theory. This material is available free of charge via the Internet at http://pubs.acs.org.

OM0702431